

Web Buckling of Steel and Composite I Girders Under Patch Load

S M Shiyekar¹, Apurva Patil², Hitesh Lahoti³

¹Professor, D Y Patil College of Engineering, Akurdi, Maharashtra State, Pune 411044, India

²Former PG Scholar, Rajarambapu Institute of, Maharashtra State, Rajaramnagar, 415414, India

³Structural Consultant and Director, Hitesh Lahoti and Associates, Maharashtra State, Pune, 411004, India

Abstract

A comparison is made between Steel I-girders and Composite I-girders under patch load conditions. The buckling phenomenon is observed using Finite Element Method (FEM), and the results are systematically compared with existing literature. The FEM results demonstrate good agreement at initial parameters. Composite materials emerge as a superior alternative to steel in plate girders. For composite web plates in I-girders subjected to patch loading, both the width of the applied load and the aspect ratio of the web plate are identified as pivotal factors influencing the buckling load.

Key Words: Steel, Composite, I Girders, Finite Element Method, ANSYS

1. Introduction

The incremental launching of steel bridges poses significant challenges, both at the construction site and in the design phase. Frequently, the structure itself faces elevated concentrated forces on the lower flange when traversing a launching shoe or an intermediate support, such as a column. These concentrated forces, commonly known as patch loads, can be substantial enough to dictate the web thickness of the bridge girder. However, even a slight increase in web thickness results in a considerable escalation in the overall steel weight of the bridge, leading to higher material costs. One potential solution to this dilemma involves enhancing the buckling resistance of the web through the incorporation of composite plates.

Ren and Tong [1] conducts a concise review of prior research on the elastic buckling of rectangular plates under simply supported and clamped boundary conditions, as well as the buckling of web plates in I-girders subjected to patch loads. Novel investigations simulate realistic loads and restraining conditions for web plates in I-girders, analyzing the buckling of numerous models with ANSYS. The study proposes formulas to predict elastic buckling coefficients accurately, accounting for rotational restraints provided by the flanges. Additionally, the paper introduces a model for assessing bearing stresses on the top edge of web plates due to wheel loads, considering crane rail rigidity. The model facilitates accurate predictions of buckling loads through suggested formulae. Chacon et al. [2] introduces a solution designed to accurately replicate the ultimate load capacity of steel plate girders under patch loading, especially when closely spaced transverse stiffeners are present. The study comprehensively describes the impact of

transverse stiffening on the ultimate load capacity. It highlights that the current formulation tends to underestimate the ultimate load capacity for girders with such geometric proportions. Numerical and theoretical comparisons affirm the accuracy of the proposed model, reinforcing and improving the current formulation. Qiao and Shan [3] focuses on pultruded fiber-reinforced plastic (FRP) composite structural shapes, analyzing local buckling of rectangular orthotropic composite plates with different edge boundary conditions. Explicit solutions for plate local buckling coefficients are obtained using a variational formulation of the Ritz method. The study treats rotationally restrained plates as discrete plates, considering elastic restraints at joint connections to analyze the local buckling of various FRP shapes under uniform axial compression. The analytical predictions align closely with experimental results and finite element analyses, proposing a design guideline for local buckling prediction and performance enhancement. Ragheb [4] introduces an analytical stability model for the local buckling of pultruded fiber-reinforced polymer (FRP) structural shapes under eccentric compression. The model treats each shape as a collection of orthotropic plates interconnected. Differential equations governing the buckling behavior of individual plates are defined and solved using Levy's solution. A parametric study using the model explores the impact of key parameters on the local buckling behavior of these shapes. Graciano and Lagerqvist [5] outlines a methodology to ascertain buckling coefficients for longitudinally stiffened plate girders under partial edge loading or concentrated loads, crucial for describing the resistance of steel plate girders. The strength curve encompasses a gradual transition from yielding to buckling, dependent on the web's slenderness ratio, a function of yield resistance to the critical buckling load ratio. Through an extensive parametric analysis, key parameters governing the shift from a global to local buckling mode are identified, with the stiffener's location and relative flexural/torsional rigidity playing significant roles. The paper concludes with an expression for the buckling coefficient, essential for determining the critical buckling load in longitudinally stiffened girder webs. The analysis of hybrid girders under patch loading has been extensively conducted by Chacon et al. [6], with a focus on girders that are transversally stiffened by the assembling plates. However, limited attention has been given to the case where girders are hybrid and simultaneously longitudinally stiffened. The motivation behind this research is to enhance the understanding of patch loading behavior, specifically for the unique structural configuration of a hybrid steel plate girder assembled with a longitudinal stiffener.

In this paper, A comparative analysis is conducted between Steel I-girders and Composite I-girders subjected to patch load conditions. Employing the Finite Element Method (FEM) [7], the buckling phenomenon is observed, and the results are compared with existing literature, demonstrating a notable agreement. Composite materials emerge as a superior alternative to steel in plate girders. In the context

of composite web plates in I-girders under patch loading, both the width of the applied load and the aspect ratio of the web plate are recognized as crucial factors influencing the buckling load.

1.1 Patch loading

A common occurrence of plate buckling involves the girder web buckling under the influence of a locally applied in-plane compressive load. In this context, "local" refers to the load not being evenly distributed across the entire width of the plate, specifically the girder web. Instances of such loading scenarios can be found in various structural applications, such as wheel loads on gantry girders, purlins on main frame structures, crane girders, and during the launching of bridge girders. In most steel structures, concentrated forces applied perpendicularly to the upper flanges of I-girders, known as patch loading, are ordinary. The reaction of a steel plate girder to patch loading can be categorized into one of three potential failure modes: yielding, buckling, and crippling, as illustrated in Fig. 1 [8]. The actual mode of failure is primarily determined by the slenderness of the web and the ratio of (where represents the thickness of the flange and represents the thickness of the web). Generally, a solid web indicates yielding failure, a slender web indicates buckling failure, and a high ratio of indicates buckling or crippling failure, while a low ratio indicates yielding failure. In practice, crippling and buckling are often entangled and challenging to distinguish. However, this combination can be supposed as a gradual shift in buckling shape as the load increases. Typically, the buckling mode initiates and is later followed by crippling at higher loads.

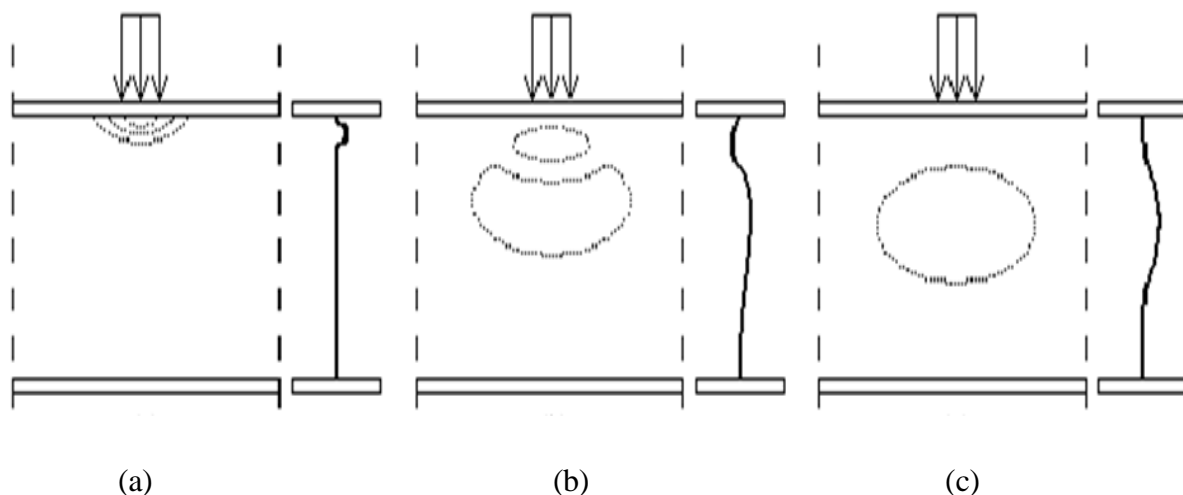


Fig. 1. Failure modes for plate girders under concentrated load. Mode (a) yielding, (b) crippling and (c) buckling. Galambos [8]

1.2 Buckling of web plate in Elastic I-girder

The elastic buckling strength of a rectangle plate under patch loading can be expressed as follow Ren and Tong [1]

$$F_{cr} = k_{cr} \frac{\pi^2 E}{12(1-\nu^2)} \frac{t_w^3}{h_w} \quad (1)$$

In the given context, the elastic buckling coefficient of the plate is denoted by k_{cr} , while h_w and t_w represent the height and thickness of the plate, respectively. Additionally, E and ν stand for the modulus of elasticity and Poisson's ratio of the material, respectively. Graciano and Lagerqvist [5] and Ren and Tong [1] proposed the following equation for the buckling coefficients of webs in I-girders under patch loading, based on numerical analysis.

$$k_{cr} = 5.82 + 2.1 \left(\frac{h_w}{a} \right)^2 + 0.46 \sqrt{\beta} \quad (2)$$

In the Eq. (2), $\beta = \frac{b_f t_f^3}{h_w t_w^3}$ represents the factor accounting for the rotational restraint exerted by the flanges.

The essence of β lies in its depiction of the ratio between the torsional stiffness of the flanges and the bending stiffness of the web. Conceptually, when β is extremely small, the rotational constraint imposed by the flanges on the web is too minimal to impede the rotation of the web itself, resulting in a behavior akin to that of simply supported plates. Conversely, as β increases, approaching infinity, the web adopts characteristics reminiscent of a clamped plate. However, the equation provided yields an infinite buckling coefficient in this scenario, which evidently contradicts the expectation of converging toward a clamped plate.

The postponement of web buckling is attributed to the existence of rotational restraint at the juncture between the flange and the web. Evaluating the elastic restraints from flanges to webs entails examining the ratio between the rotational rigidity in the flange and the bending rigidity in the web. This ratio can

be expressed as $\frac{GK}{Dh_w}$, in which, $GK = \frac{\pi^2 E}{2(1+\nu)} \frac{b_f t_f^3}{3}$ and $Dh_w = \frac{Eh_w t_w^3}{12(1-\nu^2)}$ After omitting the constant

items we get, $\beta = \frac{b_f t_f^3}{h_w t_w^3}$. Hence, it is valuable to investigate deeper into the elastic buckling behavior of

webs in I-girders under patch loading and provide a thorough explanation of the restraining effects.

2. Finite Element Analysis of Plate Girder with Patch Load

The FEM model [7] depicted in Fig. 2 is employed to analyze the buckling behavior of webs in I-girders under patch loading. The width over which the load is applied is denoted as S_s , and all nodes within the region where the load is transmitted are constrained to displace only in the vertical direction, specifically degree of freedom 2 (U_y). The patch load is transmitted through the flanges to the edges of the webs in the I-girder. To emphasize the rotational restraint provided by the flanges, a distinct model is utilized wherein the flanges and webs are established separately. In this model, only degree of freedom 2 (U_y) and 6 (U_z), i.e., the rotational about the flange-web juncture line and the out-of-plane displacement, are coupled between the flanges and web. The degree of freedom 1 (U_x) and 6 (U_z) of nodes on the left and right edges are restrained, and identical boundary conditions are applied at the edge of the flange.

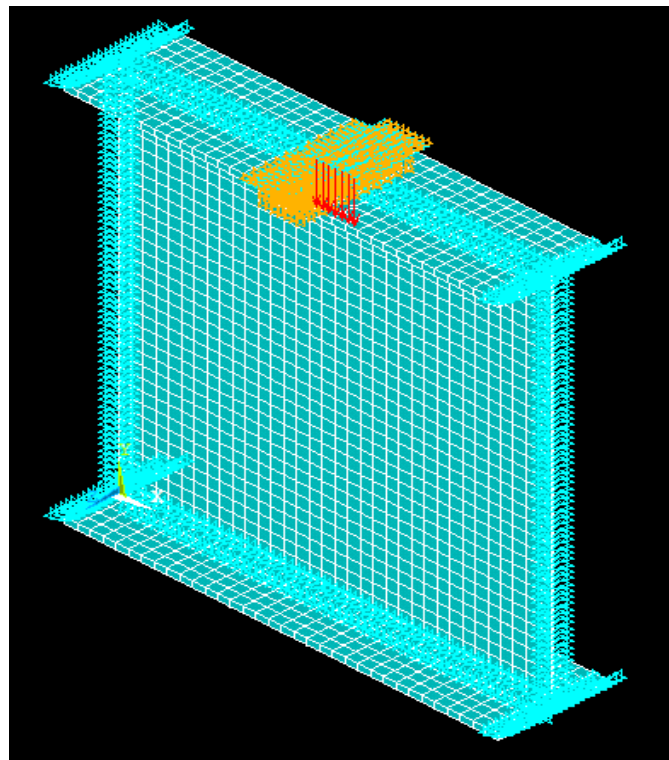


Fig. 2 The model of I-girder under patch loading with $a/h_w = 1$ with $S_s=0.1$

Results of I-girder are expressed in table 6.4.1, all dimensions for web plate, flanges ,applied load width was in table 6.4.1. Table have all results of composite web under patch loading, patch width (S_s) were 0.1 and 0.2 with simply supported boundary condition. Thickness of web in I- girder kept constant throughout analysis i.e. $t_w=0.004$. Whereas height of web $h_w=1$ m and width of flange, $b_f=0.250$. Composite material used for the analysis was boron-aluminum. Thickness of flange is calculated from β , it is different for every β value, and it plays important role in

rotational restraint to web plate. Following figure 6.4.1 and 6.4.2 show plate with aspect ratio (a/h_w) 1 and 2 respectively.

The results for the I-girder are presented in Table 1, encompassing dimensions for the web plate, flanges, and the width of the applied load. The table comprehensively includes all outcomes for the composite web under patch loading, where patch widths (Ss) were set at 0.1 and 0.2 with simply supported boundary conditions. The web thickness in the I-girder remained constant throughout the analysis, denoted as $t_w = 0.004$. The height of the web (h_w) is fixed at 1 meter, while the flange width (b_f) is set at 0.250. The composite material employed for the analysis is boron-aluminum. The thickness of the flange is calculated from β , and it varies for each β value, playing a crucial role in providing rotational restraint to the web plate. Figure 2 illustrates the plate with aspect ratios (a/h_w) of 1.

Examining Table 1, we note that for $Ss = 0.1$ and $a/h_w = 1$, the elastic buckling coefficients are significantly higher than those for $a/h_w = 2$ with the same load width of 0.1. Table 2, focusing on composite plates, reveals that for $Ss = 0.2$, the buckling coefficients are noticeably lower (almost half) compared to $Ss = 0.1$, attributed to the increased applied load width. It is evident that the web plate is more prone to buckling under larger applied load widths, resulting in an automatic decrease in the buckling load with the buckling coefficient k_{cr} .

Table 1: The elastic buckling coefficient of composite webs plate in I-girders under patch loading

$t_w = 0.004m$ $b_f = 0.250$	$h_w = 1m$	Present FEM	
		k_{cr}	
		a/h_w	
Ss	β	1.0	2.0
0.1	0.25	7.49	3.57
	1	9.72	4.92
	2	15.11	5.94
	6.75	16.68	8.73
	16	22.68	11.90
	54	36.12	18.98
	128	50.59	26.58
	0.25	2.87	1.39
	1	3.6	1.87

0.2	2	4.21	2.21
	6.75	5.80	3.10
	16	7.62	4.08
	54	11.71	6.27
	128	16.15	8.64

The crucial observation from the table above is that as β increases from 0.25 to 128, there is a corresponding rise in the elastic buckling coefficient. For $\beta = 0.25$, the web plate easily buckles because the flange thickness is minimal, equal to the web plate thickness of 0.004 meters, resulting in a buckling coefficient of 7.49. As β increases to 16, 54, and 128, corresponding to flange thicknesses of 0.016 meters, 0.024 meters, and 0.032 meters, respectively, the buckling coefficients (k_{cr}) increase to 22.68, 36.12, and 50.59. The added stiffness from the flanges for these $\beta=16, 54, 128$ values necessitate a higher buckling load for the composite web plate. The subsequent Table 2 provides a comparison between steel plates and composite plates.

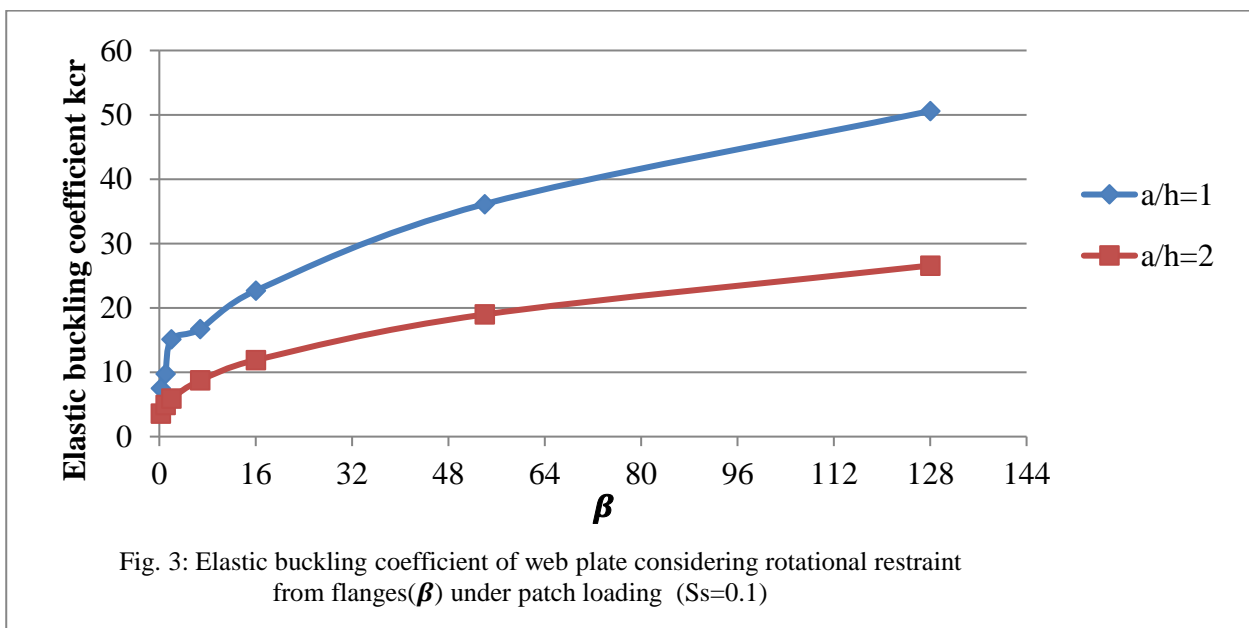
Table 2 The elastic buckling coefficient of steel webs and composite webs in I-girders under patch loading

$t_w = 0.004m$ $b_f = 0.250$	$h_w = 1m$	Present ANSYS		Ren and Tong [19]	
		Composite eb plate		Steel web plate	
		k_{cr}		k_{cr}	
Ss	β	a/h_w		a/h_w	
0.1	0.25	1.0	2.0	1.0	2.0
	1	7.49	3.57	4.33	2.90
	2	9.72	4.92	5.71	3.82
	2	15.11	5.94	6.30	4.52
	6.75	16.68	8.73	6.79	5.62
	16	22.68	11.90	6.91	6.03
	54	36.12	18.98	6.97	6.28
	128	50.59	26.58	6.99	6.34
	0.25	2.87	1.39	4.46	2.94
	1	3.60	1.87	5.86	3.88
	2	4.21	2.21	6.46	4.59

0.2	6.75	5.80	3.10	6.97	5.72
	16	7.62	4.08	7.10	6.15
	54	11.71	6.27	7.17	6.41
	128	16.15	8.64	7.18	6.47

Table 2 incorporates the results for both web plates made of steel and composite material. It is evident from the observations that the elastic buckling coefficient for the composite web plate surpasses that of the isotropic plate, or, in other words, the steel plate. For $\beta=0.25$, the buckling coefficient for the composite web plate is 7.49, while for the steel web plate, it is 4.33, highlighting a noticeable difference between these values. Similarly, at $\beta=128$, the buckling coefficient for the composite plate is 50.59, whereas for the steel web plate, it is 6.99. At $\beta=128$, the substantial difference between the composite and steel values suggests that composite material provides greater resistance to buckling compared to steel (an isotropic material). The subsequent figure elucidates the disparity between these two materials and the parameters of the plate, such as aspect ratio and thickness of the flange.

Figs. 3 and 4 provide a distinct illustration of the disparity between two aspect ratios for a composite web plate. When $a/h_w=2$, indicating a rectangular plate, it necessitates less buckling load compared to a plate with an aspect ratio of $a/h_w=1$, which represents a square composite plate. The square plate requires nearly double the buckling coefficient for plate buckling. This trend remains consistent when observing the results for an applied load width $S_s=0.2$. In this case, the only variation is the increase in applied load width, but the difference between these two aspect ratios remains the same as observed for $S_s=0.1$.



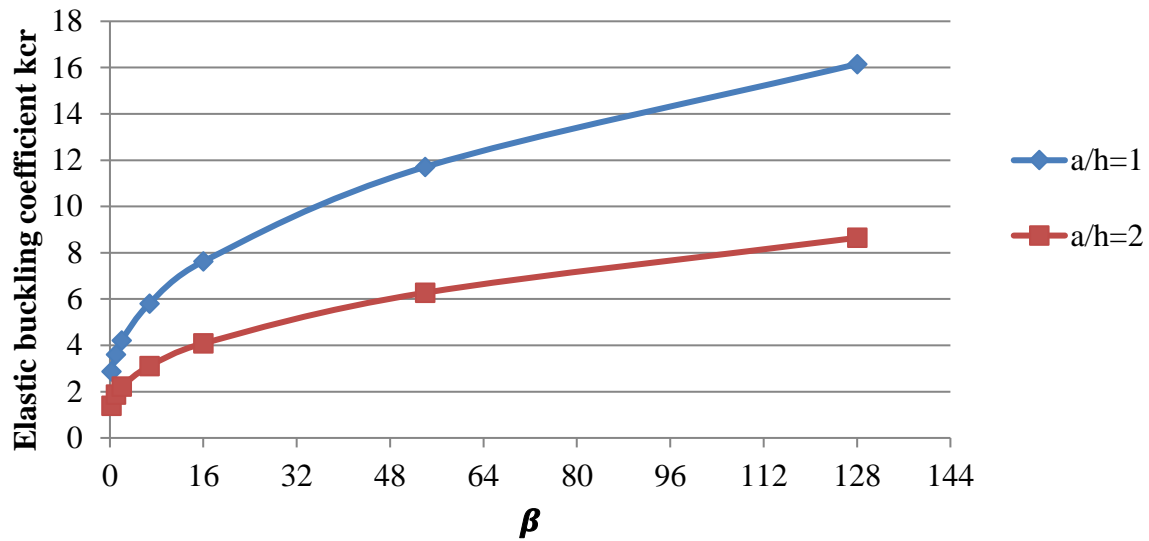


Fig. 4: Elastic buckling coefficient of web plate considering rotational restraint from flanges (β) under patch loading ($S_s=0.2$)

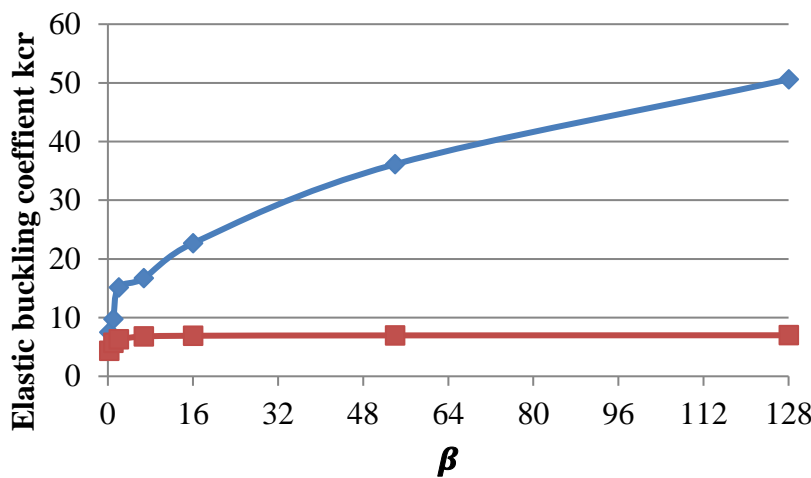


Fig. 5: Elastic buckling coefficient of steel webs & composite webs in I-girder under patch loading $S_s=0.1, a/h=1$

Figs. 5 and 6 clearly depict the elastic buckling coefficients of composite and steel web plates for $S_s=0.1$ with $a/h_w=1$ and $S_s=0.1$ with $a/h_w=2$. The discernible contrast between these two types of web plates provides insights into the stiffness of the composite material or structure. Notably, the difference in elastic buckling coefficients between these two materials exceeds double. Blue line represented by present FEM and Red by Ren and Tong [1]

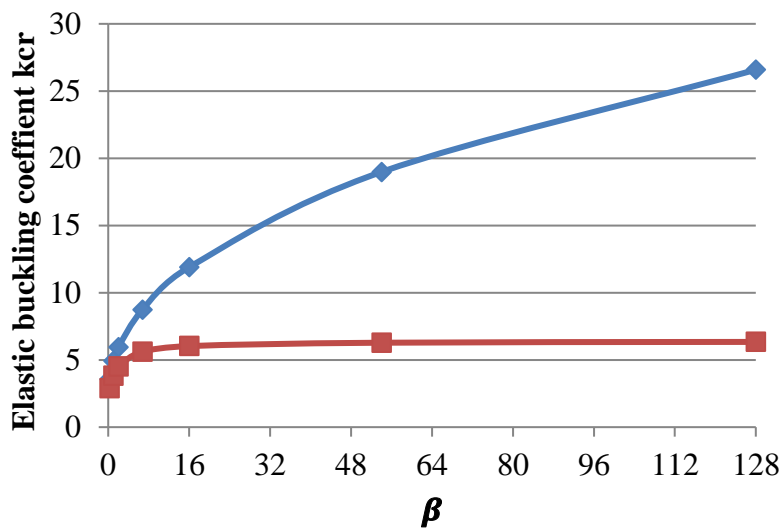


Fig. 6: Elastic buckling coefficient of steel webs & composite webs in I-girder under patch loading $S_s=0.1, a/h=2$

2.1 Deformed modes of composite web plate in I-girder

The deformed modes of the composite plate are illustrated in Fig. 7(a) and 7(b). The resistance to the buckling of the web plate is influenced by the thickness of the flange in the I-girder. Here, β represents the rotational restraint factor from the flange to the web plate. The β factor is contingent on the thickness of the flange, as evident from the stiffness of the flange to the web in the figures below. In the figures, where $\beta = 1$, deformations are observed in the flanges, while for $\beta=128$, the flanges remain undeformed, indicating a stiff behavior. When $\beta = \infty$, the plate girder acts as a clamped boundary condition.

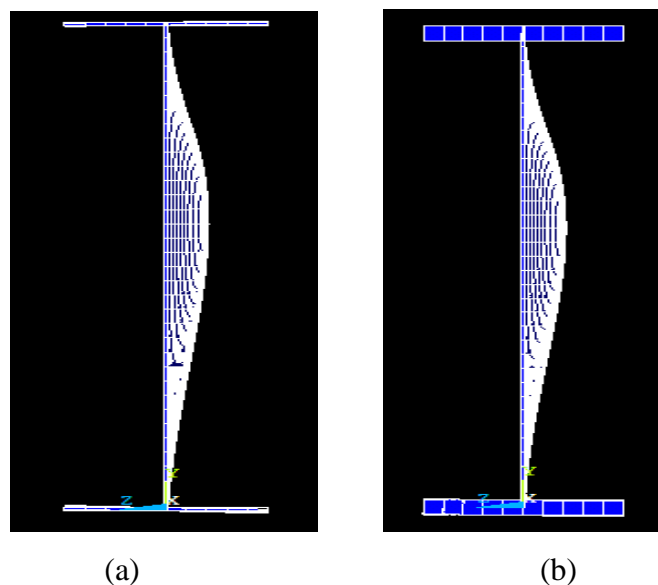


Fig. 7 a) Deformed shape of $\beta=1$ and b) $\beta=128$ of composite web plate

2.2 Buckling modes of composite web plate in I-girder

Buckling modes of composite web plate I girder are presented in the following section and first 9 mode shapes are presented in Figure 8.

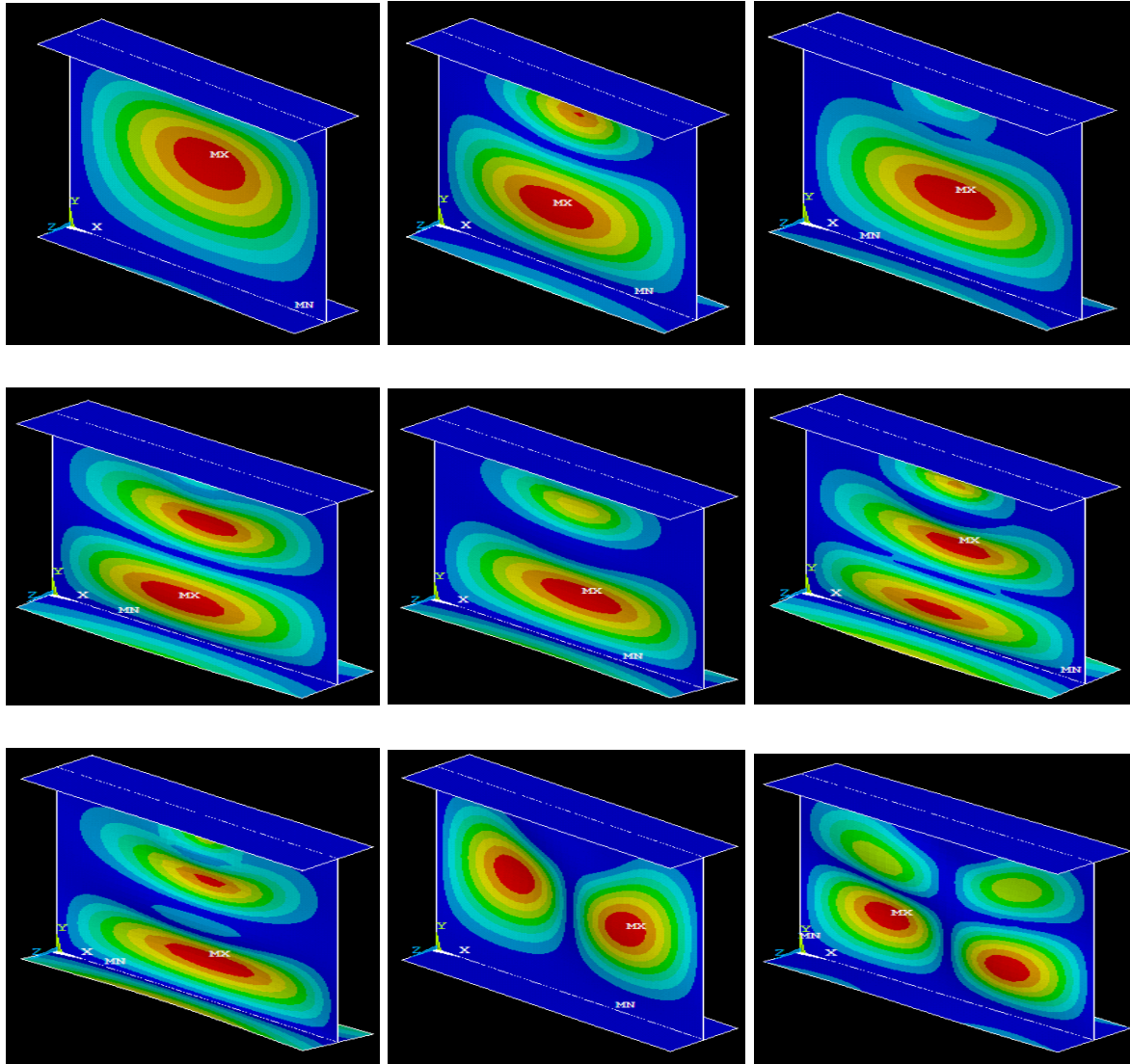


Fig. 8 First 9 Buckling Mode Shapes of composite web plate in I-girder under patch loading

3. Conclusion

In this paper, a comparative analysis is conducted between Steel I-girders and Composite I-girders under patch load conditions. Employing the Finite Element Method (FEM), the buckling phenomenon is observed, and the results are meticulously compared with existing literature, demonstrating a notable agreement. Composite materials emerge as a superior alternative to steel in plate girders. Following are some observations based on the study.

- 1) Increasing the β factor results in a thicker flange, enhancing the stiffness of the flange to the web plate, thereby leading to an increase in buckling load.
- 2) In the case of composite web plates in I-girders under patch loading, both the width of the applied load (S_s) and the aspect ratio (a/h_w) of the web plate emerge as crucial factors affecting the buckling load.
- 3) The observed elastic buckling coefficients of steel webs and composite webs in I-girders under patch loading suggest that replacing steel web plates with composite ones significantly enhances the buckling resistance of the web plate.
- 4) While steel exhibits lower corrosion resistance, composite materials boast high corrosion resistance and strength, presenting a viable alternative to steel (isotropic materials).
- 5) The comparison of the present results with existing analytical solutions indicates good agreement at initial parameters.

References

- [1] Ren T. and Tong G.S. “Elastic buckling of web plates in I-girder under patch and wheel loading”, Engineering Structures, 27, (2005), 1528-1536.
- [2] Chacon R., Mirambell E., Real E. “Transversally stiffened plate girders subjected to patch loading part 2. Additional numerical study and design proposal”, Journal of Constructional Steel Research, 80, (2013), 492-504.
- [3] Qiao P. and Shan L. “Explicit local buckling analysis and design of fiber-reinforced plastic composite structural shapes”, Composite Structures, 70, (2005), 468-483.
- [4] Ragheb W.F. “Local buckling analysis of pultruded FRP structural shapes subjected to eccentric compression”, Thin Wall Structures, 48, (2010), 709-717.
- [5] Graciano C. and Lagerqvist O. “Critical buckling of longitudinally stiffened webs subjected to compressive edge loads”, Journal of Constructional Steel Research, 59, (2003), 1119-1146.
- [6] Chacon R., Bock M. and Real E. “Longitudinally stiffened hybrid steel plate girders subjected to patch loading”, Journal of Constructional Steel Research, 67, (2011), 1310-1324.
- [7] ANSYS (2013) Standard Manual Version 13.0.